
Supporting Information

Polydopamine-Encapsulated Zinc Peroxide Nanoparticles to Target Metabolism-Redox Circuit Against Tumor Adaptability for Mild Photothermal Therapy

Yue Qiao^a, Xiaodan Jia^b, Yue Wang^b, Lin Liu^{*a}, Mengchao Zhang^{*a}, and Xiue Jiang^{*b, c}

^a Department of Radiology, China-Japan Union Hospital, Jilin University, Changchun 130033 Jilin (China)

^b Research Center for Analytical Science, College of Chemistry, Nankai University, Tianjin 300071, China

^c State Key Laboratory of Electroanalytical Chemistry, Changchun Institute of Applied Chemistry, Chinese Academy of Sciences, Changchun 130022, Jilin (China)

Emails: liulin99@jlu.edu.cn; zhangmengchao@jlu.edu.cn; xiuejiang@nankai.edu.cn

Experimental Procedures

Material. Zinc nitrate hexahydrate ($\text{Zn}(\text{NO}_3)_2 \cdot 6\text{H}_2\text{O}$, analytically pure AR), hydrogen peroxide (H_2O_2 , analytically pure AR), ammonia ($\text{NH}_3 \cdot \text{H}_2\text{O}$, analytically pure AR), ethanol (analytically pure AR), and potassium permanganate (KMnO_4 , analytically pure AR) were purchased from Xilong Chemical Co., Ltd. (Shenzhen, China). Fetal bovine serum (FBS) was purchased from Kangyuan Biotechnology Manufacturing Co., Ltd. (Tianjin, China). The low sugar DMEM culture medium, lactate dehydrogenase (LDH) activity detection kit, and α -ketoglutarate dehydrogenase (α -KGDH) activity detection kit were purchased from Solarbio Technology Co., Ltd. (Beijing, China). Dopamine hydrochloride (purity >97%), tris-(hydroxymethyl) aminomethane hydrochloride (Tris HCL) (purity $\geq 99.0\%$), polyethylene imine (PEI-10000, purity $\geq 99.0\%$), tris-(2-Carboxyethyl) phosphin hydrochloride (TCEP), fluorescein isothiocyanate isomer I (FITC), ammonium formate and zincon (ZI) were purchased from Aladdin Reagent Co., Ltd. (Shanghai, China). Catalase (CAT) was purchased from Sigma Aldrich (Shanghai, China). Calcein acetoxymethyl ester (AM), propyrium Iodide (PI), 2',7'-dichlorofluorescein diacetate (DCFH-DA), Dihydroethidium (DHE), mitochondrial membrane potential detection kit (JC-1), glucose detection kit, NAD^+/NADH detection kit, enhanced ATP detection kit, GSH and GSSH detection kit, HSP 70 antibody (mouse monoclonal antibody), β -Actin antibody (mouse monoclonal antibody) and horseradish peroxidase labeled goat anti mouse IG were purchased from Beyotime Biotechnology Co., Ltd. (Shanghai, China). Tetrakis-(2-pyridylmethyl) ethylenediamine (TPEN) was purchased from

Macklin Biochemical Technology Co., Ltd. Zinquin ethyl ester was purchased from Maokang Biotechnology Co., Ltd. Phosphate buffer solution (PBS) was purchased from Bioss Biotechnology Co., Ltd. The enhanced cell counting kit-8 (CCK-8) reagent kit was purchased from Yamei Biopharmaceutical Technology Co., Ltd. (Shanghai, China). High sugar DMEM culture medium was purchased from Thermo Fisher Technology Co., Ltd. The lactate content detection kit was purchased from Beibo Biotechnology (Shanghai, China). Purified rabbit liver metallothionein-1 (MT-1) was purchased from Enzyme Linked Biotechnology Co., Ltd. (Shanghai, China). All experimental water was ultrapure water. All reagents were used directly after purchase.

Instruments. The nanoparticle morphology was observed using H-600 transmission electron microscopy (Hitachi, Japan). The dynamic laser scattering (DLS) was performed by ZEN3690 Zetasizer (Marvin, UK). The UV-Vis absorption spectrum was obtained using a UV-Vis spectrometer UV-1700 (Shimadzu, Japan). X-ray diffraction analysis (XRD) was carried out using a Bruker D8 advanced X-ray diffractometer (CuK α radiation, Germany). The metal particle concentration was measured using an inductively coupled plasma atomic emission spectrometer (ICP-AES, Thermo Fisher Science, USA). X-ray photoelectron spectroscopy (XPS) performed by ESCALAB Xi+ electron spectrometer (Thermo Scientific, USA). Fluorescence images were captured using confocal laser scanning microscopy A1 (Nikon, Japan). CCK-8 analysis was analyzed using the microplate reader (Bio-Tek, USA).

Methods

Synthesis of ZnO₂ NPs. Initially, 10 mL of 0.1M Zn (NO₃) · 6H₂O aqueous solution was added into PEI aqueous solution (10 mg mL⁻¹, 20 mL) and stirred for 20 min. And then, 3 mL of 1 M NH₃ · H₂O was added into the above solution with continue stirring for 20 min. Finally, 0.4 mL of 30% H₂O₂ was slowly dripped into the above solution and then stirred for 4 h at room temperature. The ZnO₂ NPs were collected through centrifugation at a speed of 10,000 rpm for 10 min, washed with water, and then stored in a 4°C refrigerator.

Synthesis of ZnO₂@PDA NPs. Briefly, 13 mg of the as-prepared ZnO₂ NPs was dissolved in 65 mL of Tris HCL buffer solution (pH 8.5) under ultrasound for 10 min. Then, 26 mg of tryptone was added into the above solution and stirred for 20 min. Finally, 26 mg of dopamine hydrochloride was added with continue stirring for 12 h at room temperature. The ZnO₂@PDA NPs were obtained after centrifugation and washing. The content of PDA was calculated by thermogravimetry (TG).

Synthesis of FITC-labeled ZnO₂@PDA NPs. ZnO₂@PDA NPs (10 mg) was dissolved into 9 mL of aqueous solution, 1 mL of FITC aqueous solution (1 mg mL⁻¹) was added into the above solution, and the mixture was allowed to react for 12 h at room temperature. At last, the FITC-labeled ZnO₂@PDA NPs were obtained after centrifugation and washing.

Synthesis of PDA NPs. The PDA NPs were prepared by the previously reported method.¹ In brief, 5 mL

of 0.1 M NaOH solution and 55 mL of anhydrous ethanol were added into 130 mL of water under continuous stirring. Subsequently, 190 mg of dopamine hydrochloride was added and stirred for 24 h. The PDA NPs were collected through centrifugation and washing.

Colorimetric Assay of Peroxo Groups. The aqueous solution containing $50 \mu\text{g mL}^{-1}$ KMnO_4 and 0.1 M H_2SO_4 was treated with ZnO_2 NPs or $\text{ZnO}_2@\text{PDA}$ NPs. The UV-vis spectra were measured from 400 to 650 nm.

The pH-Responsive Decomposition of $\text{ZnO}_2@\text{PDA}$ NPs. The acid-induced dissociation was assessed by measuring Zn^{2+} and H_2O_2 release. Briefly, 5 mL of $\text{ZnO}_2@\text{PDA}$ NPs were placed in a dialysis bag, then suspended in 30 mL PBS buffer solution (pH 5.5 and 7.4), and shaken evenly at 37°C . At varied time points, a 2 mL sample of buffer solution was taken and the solution was replenished with 2 mL of fresh buffer. The samples were used to examine the Zn^{2+} and H_2O_2 concentrations. Zn^{2+} concentration was detected by ICP-MS. The H_2O_2 concentration was measured by cerium sulfate method.²

Photothermal Performance of $\text{ZnO}_2@\text{PDA}$ NPs. To assess the photothermal performance of $\text{ZnO}_2@\text{PDA}$ NPs, 1 mL of $\text{ZnO}_2@\text{PDA}$ NPs solutions with different concentrations was put into a 3 mL quartz cell and then subjected to laser irradiation (808 nm , 1.0 W cm^{-2}) for 10 min. Temperature changes were detected by a thermocouple probe and recorded every 30 seconds. Infrared thermal images were captured every 2 min. The same approach was employed to assess the photothermal performance under varying irradiation laser power densities.

To assess the photothermal performance of $\text{ZnO}_2@\text{PDA}$ NPs after degradation, $\text{ZnO}_2@\text{PDA}$ NPs ($150 \mu\text{g mL}^{-1}$) were dispersed in PBS buffer solution (pH 5.5) for various time periods, and then subjected to laser irradiation (808 nm , 1.0 W cm^{-2}) for 10 minutes. The temperature of $\text{ZnO}_2@\text{PDA}$ NPs solution was measured by the same method as above.

To investigate the photothermal stability of $\text{ZnO}_2@\text{PDA}$ NPs, 1 mL of $\text{ZnO}_2@\text{PDA}$ NPs solution ($200 \mu\text{g mL}^{-1}$) was irradiated upon the 808 nm laser (1.0 W cm^{-2}) for 15 min. Subsequently, the laser was turned off, and the sample was allowed to cool naturally to its initial temperature. This operation was repeated four times.

In order to investigate the photothermal conversion efficiency, 1 mL of $\text{ZnO}_2@\text{PDA}$ NPs solution ($200 \mu\text{g mL}^{-1}$) was subjected to laser irradiation (808 nm , 1.0 W cm^{-2}) for 15 min. The laser was then turned off and the solution was allowed to cool naturally. The photothermal conversion efficiency was worked out by the previously reported method.³

Cytotoxicity Experiment. Hela cells and Human umbilical vein endothelial cells (HUVEC) were inoculated onto a 96-well plate with a density of 5×10^3 cells per well, and incubated in the condition of 37°C and 5 % CO_2 for 24 h. In order to simulate the nutrient deficient microenvironment of tumors, Hela was cultured in low sugar DMEM and HUVEC cells were cultured in high sugar DMEM. And then the

culture medium was replaced with corresponding DMEM containing different concentrations of ZnO₂@PDA NPs. The cells were further cultured for 24 h. Subsequently, the wells were washed three times with PBS and then 100 μL of CCK-8 solution was added to the wells for 1 h of treatment. Finally, the absorbance of each well was measured at 450 nm to detect the cell survival rate.

Photothermal Effects at The Cellular Level. HeLa cells were seeded into 96-well plates and incubated at 37 °C in 5% CO₂ for 24 h. Then the medium was replaced with fresh DMEM, PDA (20.7 μg mL⁻¹ in fresh DMEM medium), ZnO₂@PDA NPs (150 μg mL⁻¹ in DMEM medium) for 24 h. And then each well of the laser groups was subjected to 808 nm laser irradiation (1.0 W cm⁻²) for 10 min. The cell survival rate was tested using the CCK-8 assay.

Intracellular Uptaken of FITC-labeled ZnO₂@PDA NPs. The uptaken of FITC-labeled ZnO₂@PDA NPs in the HeLa cell was detected through the variation of fluorescence of FITC with the help of CLSM using an excitation of 488 nm. Basically, HeLa cells were cultured in the 20 mm wells of a glass bottom cell culture dish (1 × 10⁵ cells per dish) for 24 h. Then, HeLa cells were incubated with FITC-labeled ZnO₂@PDA NPs (200 μg mL⁻¹) for another 1, 2 and 4 h. After that, each culture dish was rinsed with PBS for three times and detected by CLSM.

Detection of Intracellular Zinc Ions and Reactive Oxygen Species. The levels of intracellular free Zn²⁺, H₂O₂, and ·O₂⁻ were detected by Zinquin ethyl ester, DCFH-DA, and DHE, respectively. Basically, HeLa cells were cultured in the 20 mm wells of a glass bottom cell culture dish (1 × 10⁵ cells per dish) for 24 h. After removal of the culture medium, the cells were incubated with DMEM, PDA (20.7 μg mL⁻¹ in fresh DMEM medium), ZnO₂@PDA NPs (150 μg mL⁻¹ in DMEM medium), ZnO₂@PDA NPs + TPEN (a total of 4 μM in two batches), ZnO₂@PDA NPs + CAT (50 μg mL⁻¹) for another 4 h. Then, the medium was discarded, and the cells were washed twice with PBS, and stained with PBS containing probes (Zinquin ethyl ester at 20 μM, DCFH-DA at 10 μM, DHE at 10 μM) according to the instructions. Finally, Intracellular levels of Zn²⁺, H₂O₂, and ·O₂⁻ were observed by CLSM.

The Effect of H₂O₂ on the release of Zn²⁺ from MTs. To determine the effect of H₂O₂ on the release of Zn²⁺ from MTs, zinc indicator ZI was used to detect free Zn²⁺, as ZI can chelate free Zn²⁺ and form an absorption peak at 618 nm. 0.5 mg of MTs was dissolved in 450 μL of ammonium formate buffer (pH 7.4) containing 0.5 mM TCEP and 0.8 mM ZI with or without 5 μL of 0.27 M H₂O₂. The absorbance curves from 580 to 680 nm at different time points were recorded. The curve of 0 min was detected before adding H₂O₂. The positive control was prepared using 5 μM zinc acetate with 60 μM of ZI in ammonium formate buffer (pH 7.4).

Detection of Mitochondrial Membrane Potential. HeLa cells were cultured in the 20 mm wells of a glass bottom cell culture dish (1 × 10⁵ cells per dish) for 24 h. Then the medium were replaced with DMEM, PDA (20.7 μg mL⁻¹ in fresh DMEM medium), ZnO₂@PDA NPs (150 μg mL⁻¹ in DMEM

medium), ZnO₂@PDA NPs + TPEN (a total of 4 μM in two batches), ZnO₂@PDA NPs + CAT (50 μg mL⁻¹) for another 4 h incubation before removal of the culture medium. The cells were washed twice with PBS, and exposed to JC-1 probe for 20 min according to the instructions. Images were captured using CLSM.

Living and dead cell co-staining experiment. In brief, HeLa cells were cultured in culture dishes and incubated for 24 h. Then HeLa cells were subjected to various treatments for an additional 24 h, and the cells of laser groups were subjected to 808 nm laser irradiation (1.0 W cm⁻²) for 10 min. The cells were co-stained with calcein AM (40 nM) and PI (4.5 μM) in PBS for 30 min and observed by CLSM.

Analysis of Regulation in Glycolysis and Mitochondrial Respiration. To detect NADH and ATP content, HeLa cells were seeded into 6-well plates at a density of 2×10⁵ cells per well and incubated for 24 h. Then, they were subjected to various treatments for an additional 24 h. The cells were harvested to quantify the levels of NADH and ATP using reagent kits.

To assess LDH activity and α-KGDH activity, HeLa cells were seeded into 100 mm culture dishes at a density of 1×10⁶ cells per dishes and incubated for 24 h. Then, they were subjected to various treatments for an additional 8 h. The cells were harvested to quantify the LDH activity, α-KGDH activity using reagent kits.

To detect the glucose and lactic acid content in the culture medium, HeLa cells were seeded into 12-well plates at a density of 1×10⁵ cells per well and incubated for 24 h. Then, they were subjected to different formulations within DMEM medium for an additional 24 h. And the supernatant of medium after centrifugation was collected and treated with lactic acid assay kit and glucose assay kit.

Detection of Intracellular Glutathione. To detect GSH, HeLa cells were cultured on 6-well plates and incubated for 24 h. Then, they were subjected to various treatments for 24 h. The cells were harvested to quantify the intracellular levels of glutathione content using an assay kit following the instructions provided.

Western Blot Analysis. To assess the expression of HSP 70, HeLa cells were cultured in 6-well plates. The experiment was divided into six groups. (1) PBS; (2) PBS + laser (808 nm, 1.0 W cm⁻², 10 min); (3) PDA NPs; (4) PDA NPs + laser; (5) ZnO₂@PDA NPs; (6) ZnO₂@PDA NPs + laser. Subsequently, the cells were collected after washed, and lysed using RIPA lysis buffer. And the supernatant after centrifuged was collected for quantitative protein level analysis and Western blot analysis. In brief, the obtained protein samples separated by sodium dodecyl sulfate-polyacrylamide gel electrophoresis (SDS-PAGE) were isolated and transferred onto polyvinylidene fluoride (PVDF) membranes. After blocking for 1 hour with 5% BSA, the membrane was incubated with anti-HSP70, horseradish peroxidase conjugated secondary antibodies in turn. Finally, the membrane was visualized by the ECL plus detection system.

Animal Models. All animal experiments were operated in accordance with the guidelines for ethical

review of animal welfare (GB/T 35892-2018) and approved by the Institutional Animal Care and Use Committee (IACUC) of Changchun institute of Applied Chemistry, Chinese Academy of Sciences (IACUC issue NO. CIAC 2023[0173]). The female Kunming mice (6 weeks old, weighing 20-25 g) were subcutaneously injected with 1×10^6 uterine cervical cancer cells (U14) in 100 μ L PBS solution in the right abdomen.

Thermal Imaging of Tumor Sites *in Vivo*. After intravenous injection of ZnO₂@PDA NPs (25 mg kg⁻¹) at different times, the tumor site was exposed to an 808 nm laser (1 W cm⁻²) for 10 min. The photothermal imaging was recorded using an infrared thermal imaging camera.

Anti-Tumor Effects *in Vivo*. Tumor-bearing mice were randomized into six groups after the tumor grew to about 80 mm³: (1) PBS; (2) PBS + laser; (3) PDA NPs (3.5 mg kg⁻¹); (4) PDA NPs + laser; (5) ZnO₂@PDA NPs (25 mg kg⁻¹); (6) ZnO₂@PDA NPs + laser. Tumor-bearing mice were injected through tail vein on the first, third, and fifth days. At 12 h post-injection, the tumor area of the laser groups was irradiated with 808nm laser (1 W cm⁻²) for 5 min. The body weight and tumor size were recorded every two days. Tumor volume (V) was calculated using the following equation: $Volume = (Length \times Width^2)/2$. On the 15th day, all mice were euthanized. Blood was taken from the orbit for blood routine and biochemical analysis testing. The tumor tissue, heart, liver, spleen, lungs, and kidneys were dissected. All tissues were fixed with 4% buffered paraformaldehyde for histological examination.

Histological Examination. The main tissue sections were stained with hematoxylin and eosin (H&E). The tumor sections were stained with H&E, HSP 70 and TUNEL antibodies.

Statistical Analysis. The results were presented as the mean with standard deviation (S.D.). The differences between the two groups were assessed using a student T-test. The level of significance was set at $P < 0.05$.

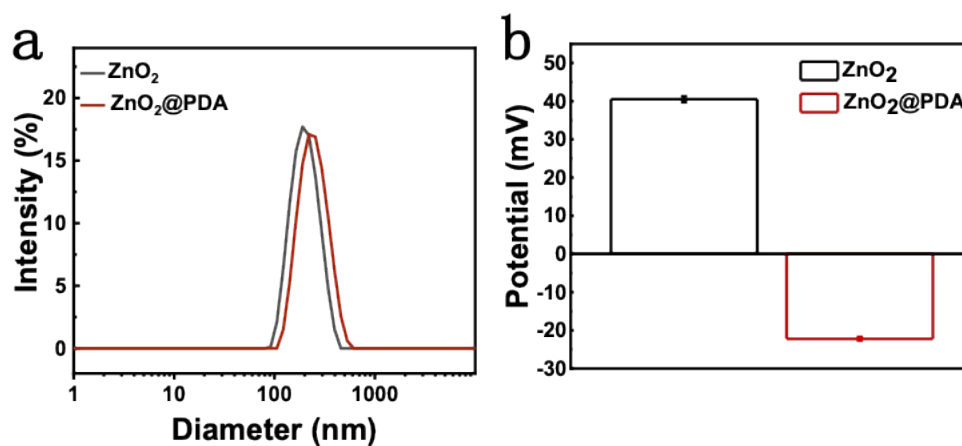


Figure S1. (a) Hydrodynamic sizes of ZnO₂ and ZnO₂@PDA NPs. (b) Zeta potentials of ZnO₂ and ZnO₂@PDA NPs.

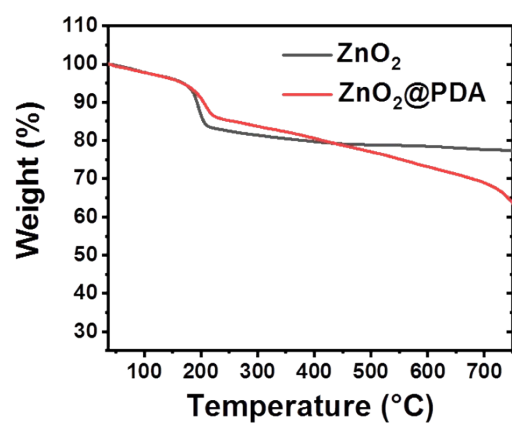


Figure S2. Thermogravimetric analysis of ZnO₂ and ZnO₂@PDA NPs.

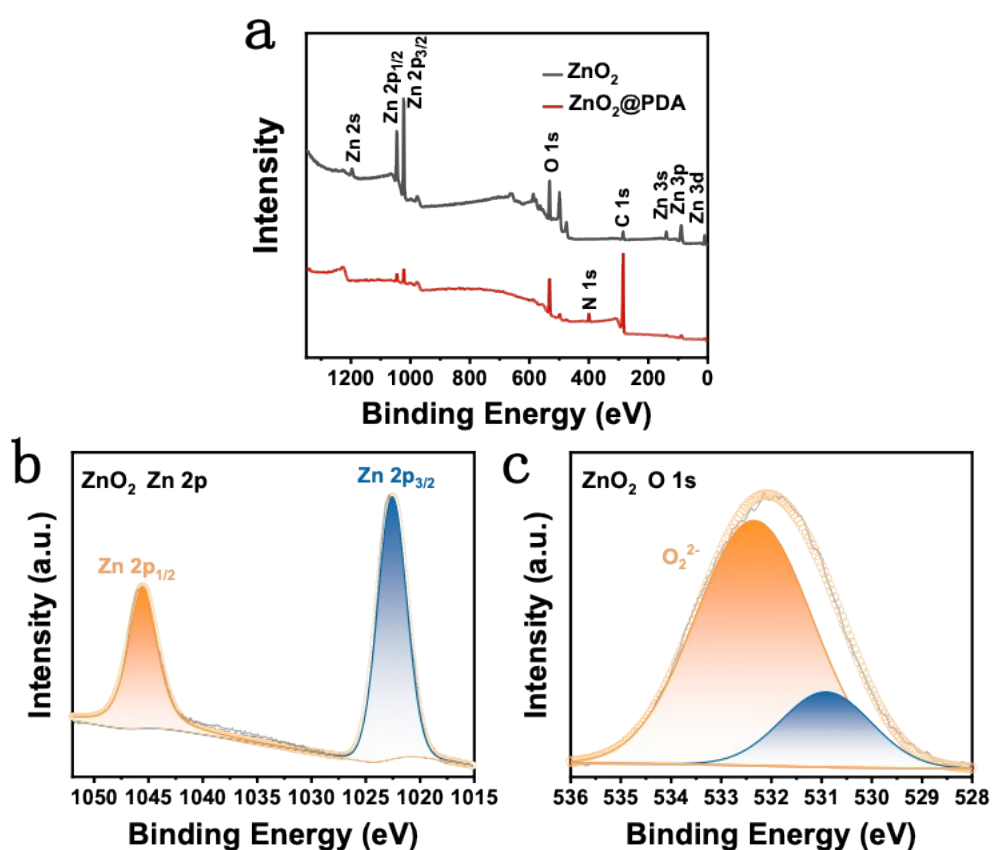


Figure S3. (a) XPS survey spectra of ZnO_2 and $\text{ZnO}_2@\text{PDA}$ NPs. (b-c) XPS spectra of ZnO_2 NPs: Zn 2p regions (b) and O 1s regions (c). The peak in the Zn 2p orbital spectrum at 1045.6 eV was identified as Zn $2p_{1/2}$, while the peak at 1022.6 eV was associated with Zn $2p_{3/2}$; The peak at 532.4 eV in the O1s orbital spectrum could be attributed to O_2^{2-} , indicating successful synthesis of ZnO_2 NPs.

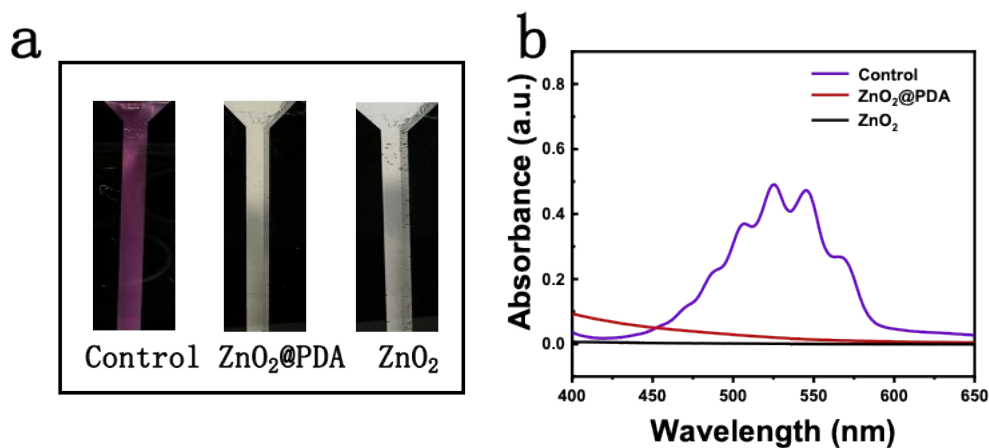


Figure S4. (a-b) KMnO_4 colorimetric analysis to prove the existence of peroxy groups in ZnO_2 and ZnO_2 @PDA NPs. Besides. The presence of peroxy groups could reduce pink MnO_4^- to colorless Mn^{2+} .

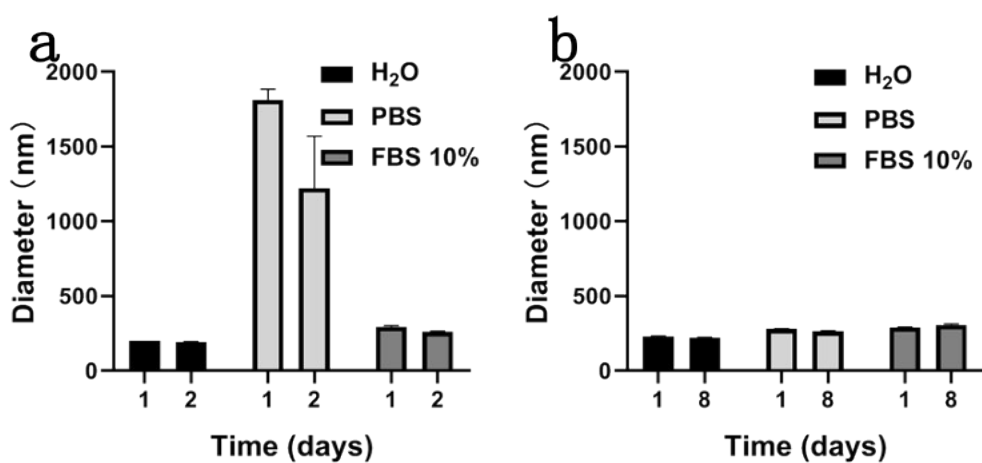


Figure S5. Hydrodynamic size distribution after incubation with ZnO_2 NPs (a) and ZnO_2 @PDA NPs (b) in water, PBS, or 10% FBS. Data are represented as mean \pm S.D.

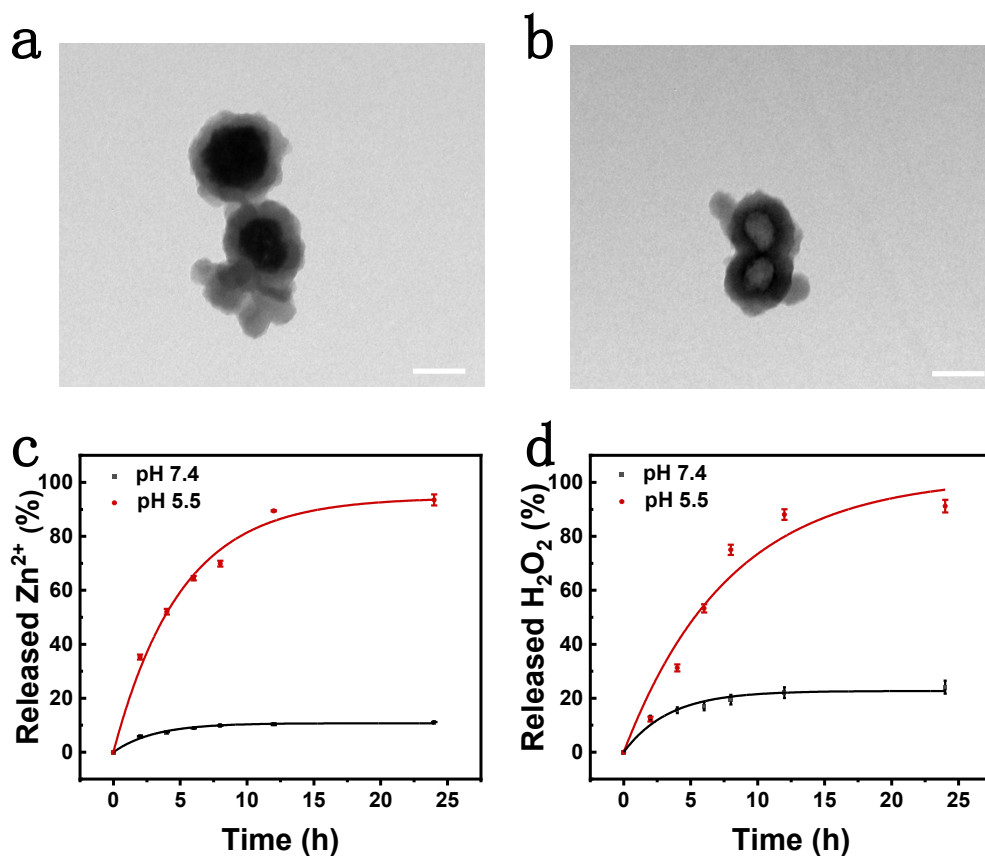


Figure S6. (a, b) TEM images of ZnO₂@PDA NPs after 12 h of incubation in PBS buffer solutions: pH 7.4 (a) and pH 5.5 (b). Scale bar: 100 nm. (c) Zn²⁺ and (d) H₂O₂ release profiles from ZnO₂@PDA NPs in different pH buffers. Data are represented as mean ± S.D. n = 3. Zn²⁺ concentration was detected by ICP-MS. The H₂O₂ concentration was measured by cerium sulfate method, as Ce⁴⁺ can be reduced to colorless Ce³⁺ by H₂O₂ in acid solution.

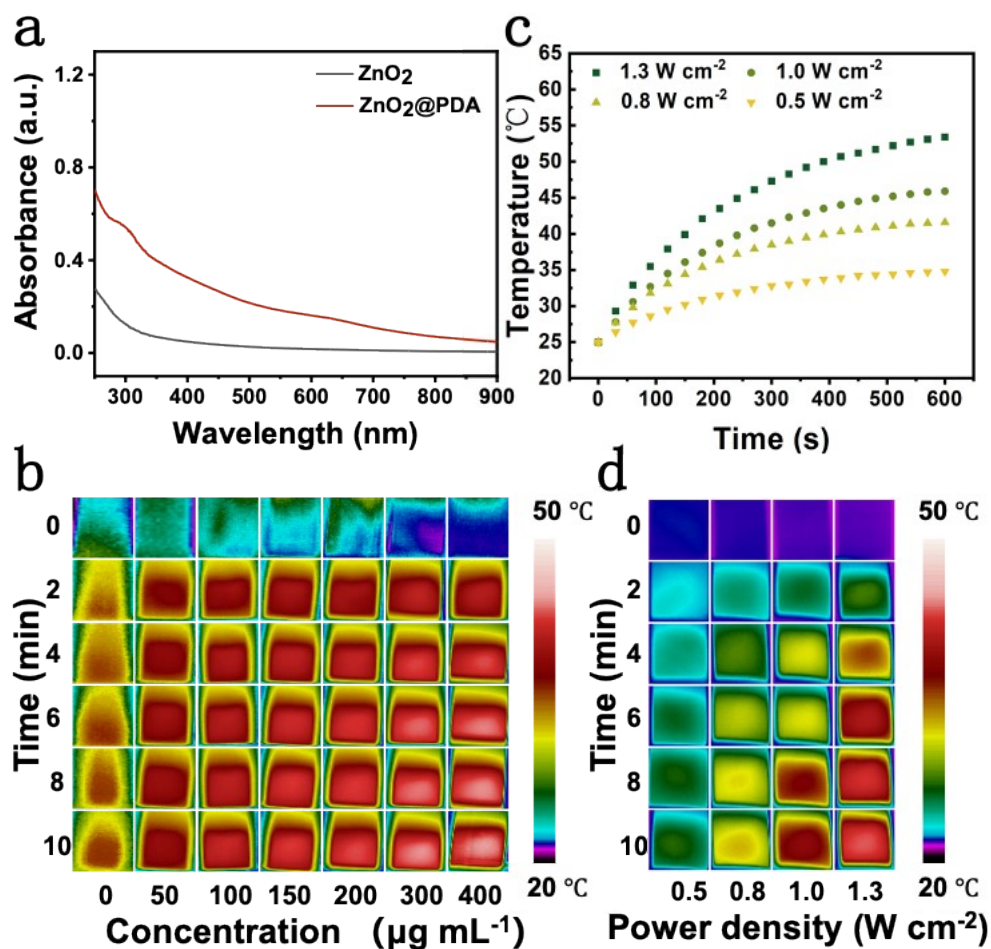


Figure S7. (a) UV-vis absorption spectrum of ZnO₂ NPs and ZnO₂@PDA NPs. (b) Thermographic images of ZnO₂@PDA NPs at different concentrations upon 808 nm laser exposure (1.0 W cm⁻²). (c) Photothermal heating curves of ZnO₂@PDA NPs (200 μg mL⁻¹) upon 808 nm laser exposure with different power densities. (d) Thermographic images of ZnO₂@PDA NPs upon 808 nm laser exposure with different power densities.

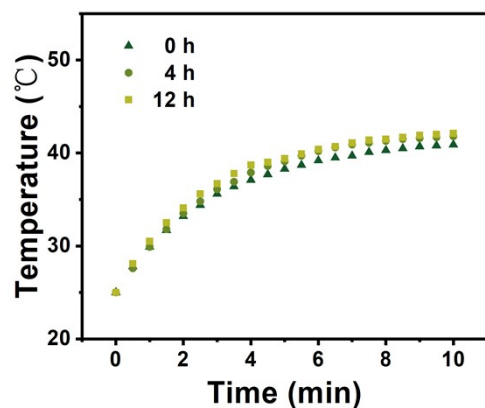


Figure S8. After incubation with PBS buffer solution (pH 5.5) for 0, 4 and 12 h, the heating curves of ZnO₂@PDA NPs (150 μg mL⁻¹) upon 808 nm laser exposure (1.0 W cm⁻²).

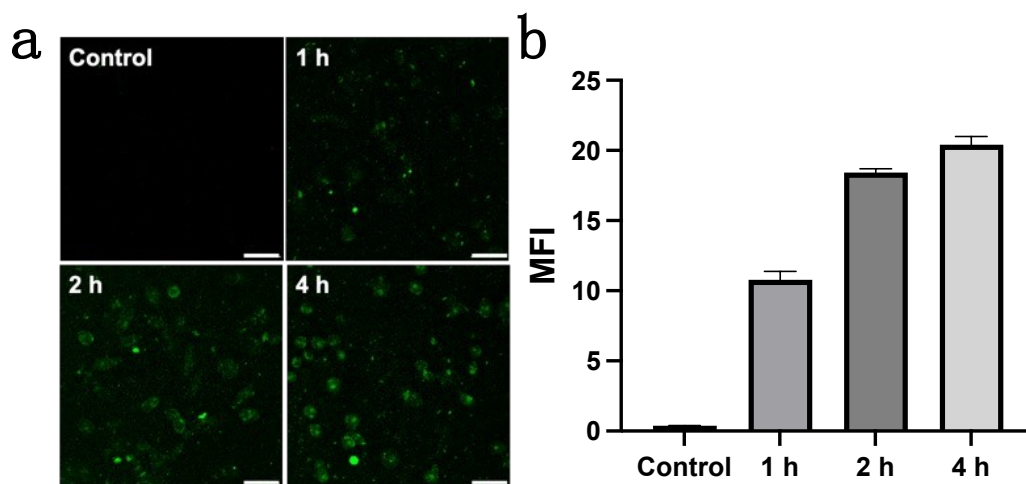


Figure S9. (a) CLSM images of HeLa cells incubated with FITC-labeled ZnO₂@PDA NPs (Green) at different culture time points. The scale bar is 50 μm. (b) According to (a), the relative the MFI (mean fluorescence intensity) of intracellular uptake in HeLa cells at different culture time points.

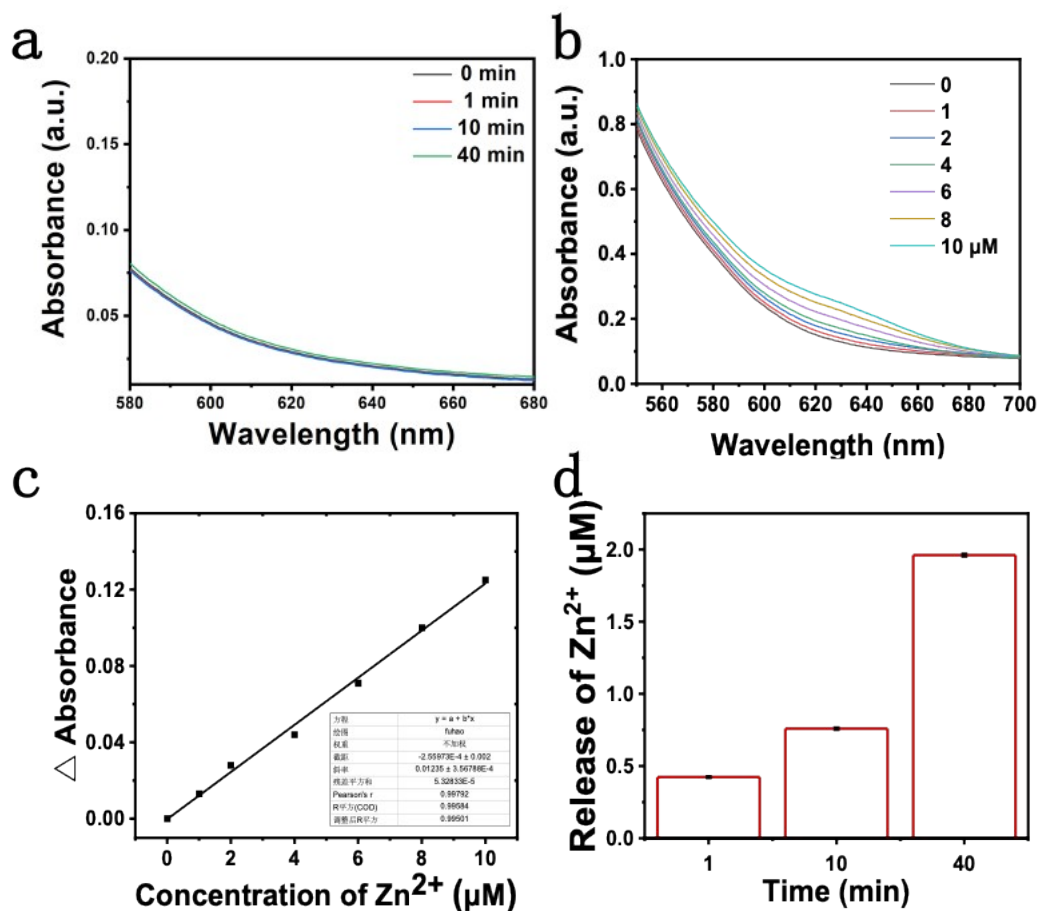


Figure S10. (a) Absorption spectra showing the release of Zn^{2+} from MTs without H_2O_2 . ZI was used as Zn^{2+} indicator, which can chelate free Zn^{2+} to form an absorption peak at 618 nm. The results showed that there was no significant absorbance increase at 618nm in the absence of H_2O_2 , indicating that Zn^{2+} were almost not released from MTs. (b) UV-vis absorption spectra of Zn^{2+} with different concentrations in ammonium formate buffer (pH 7.4) containing 0.5 mM TCEP and 0.8 mM ZI. (c) Standard curve of the Zn^{2+} . (d) The release of Zn^{2+} from MTs in the presence of H_2O_2 .

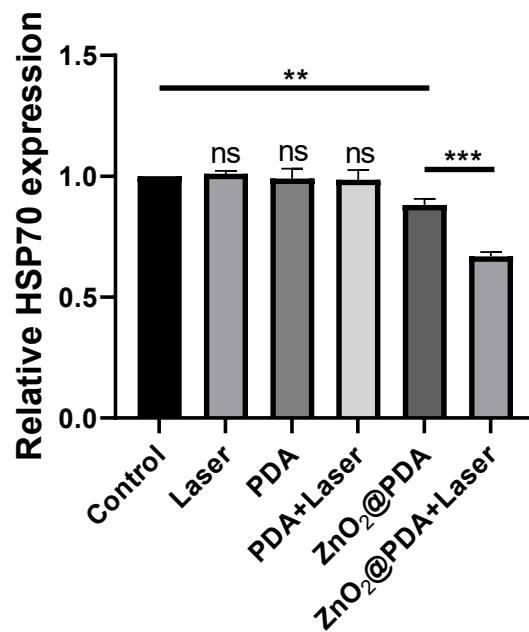


Figure S11. According to Figures 3e, the relative expression level of HSP 70 in HeLa cells subjected to diverse treatments for 24 h. ** $P < 0.01$, *** $P < 0.001$.

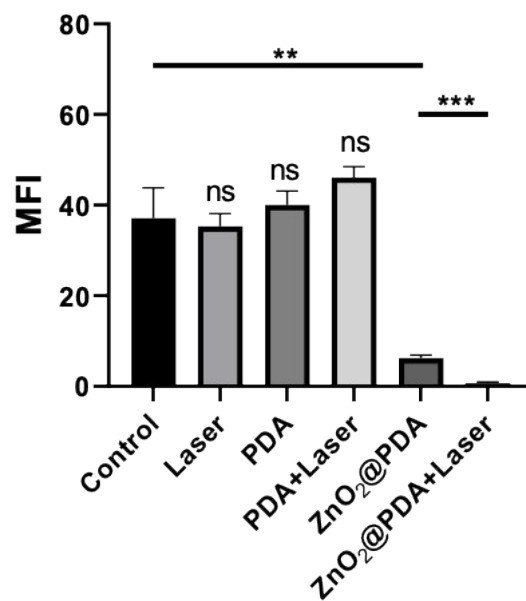


Figure S12. According to Figures 3g, the MFI of Calcein AM (Green color represents live cells) in the fluorescence images. $**P < 0.01$, $***P < 0.001$.

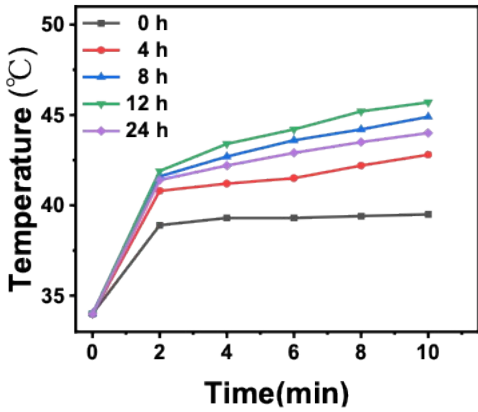


Figure S13. Heating curves of tumor sites after intravenous injection under laser irradiation monitoring through infrared thermal imaging camera.

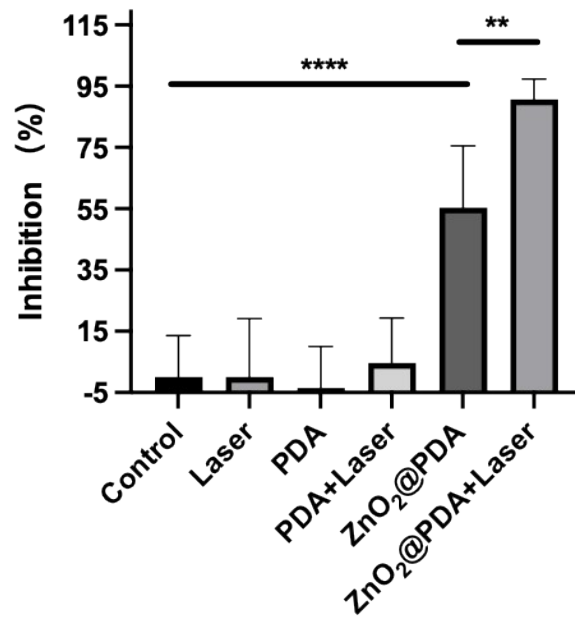


Figure S14. The tumor inhibition rate of all groups. The tumor inhibition of the control group is considered to be zero. $**P < 0.01$, $****P < 0.0001$.

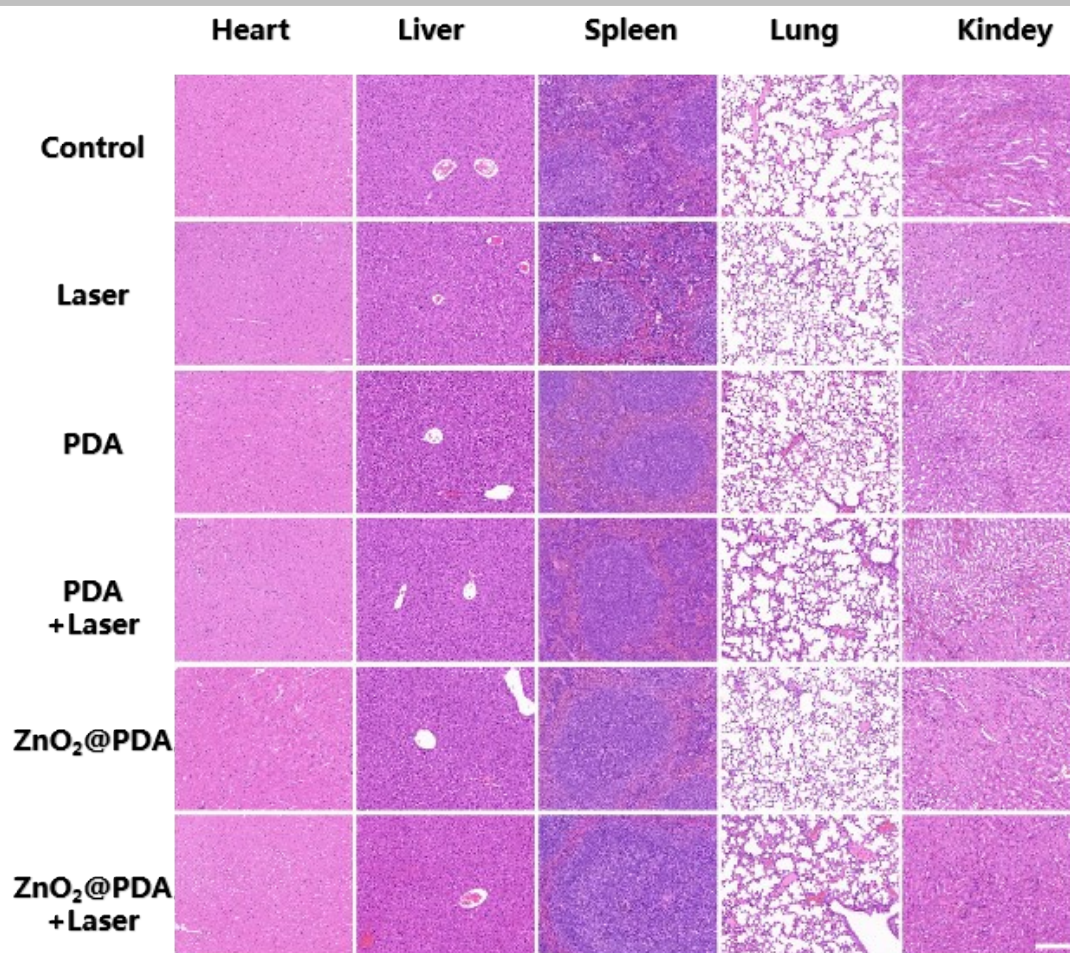


Figure S15. H&E staining images of major organs of mice treated with different treatments. The scale bar is 200 μm .

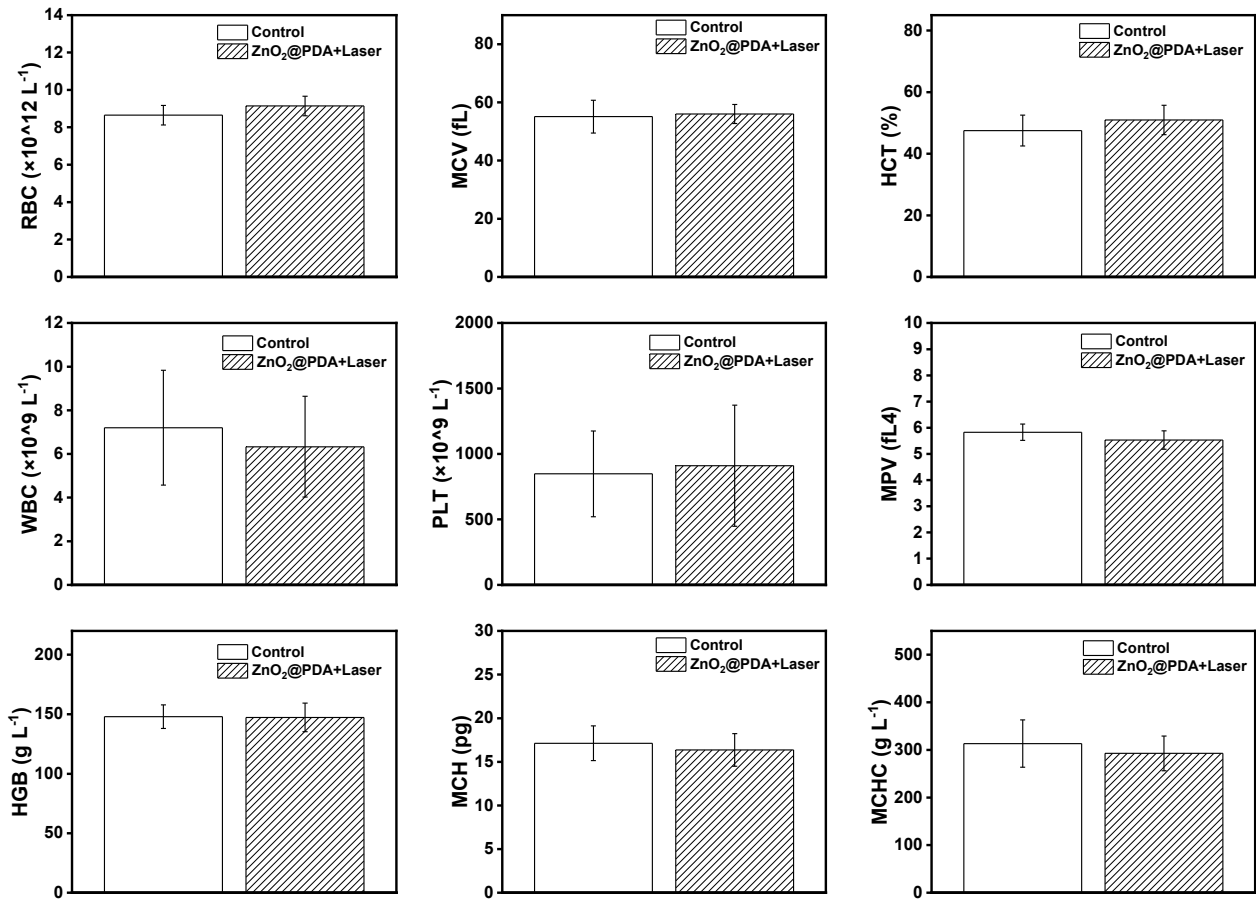


Figure S16. Hematology analysis of whole-blood parameters in mice with different treatments. Data are represented as mean \pm S.D.

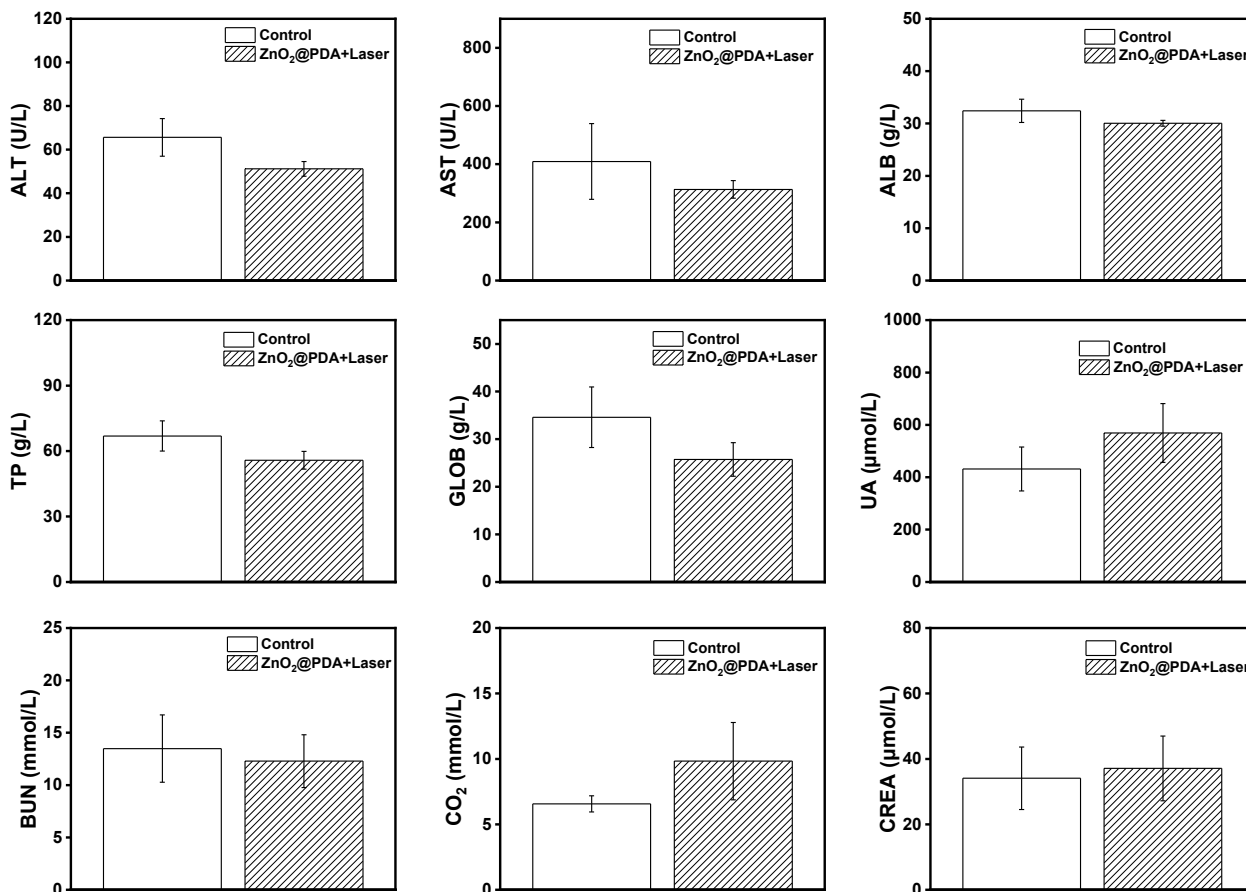


Figure S17. The levels of liver and renal indicators in mice with different treatments. Data are represented as mean \pm S.D.

References

1. M. Wu, T. Wang, L. Müller and F. A. Müller, *Colloids and Surfaces A: Physicochemical and Engineering Aspects*, 2020, **603**.
2. M. Zhang, R. Song, Y. Liu, Z. Yi, X. Meng, J. Zhang, Z. Tang, Z. Yao, Y. Liu, X. Liu and W. Bu, *Chem*, 2019, **5**, 2171-2182.
3. D. K. Roper, W. Ahn and M. Hoepfner, *The Journal of Physical Chemistry C*, 2007, **111**, 3636-3641.